



Low-cycle fatigue behavior of a directionally solidified Ni-based superalloy subjected to gas hot corrosion pre-exposure

Hong-Yu Qi, Ji-Shen Yang, Xiao-Guang Yang* , Shao-Lin Li

Received: 19 August 2015 / Revised: 9 November 2015 / Accepted: 19 December 2016 / Published online: 10 March 2017
© The Nonferrous Metals Society of China and Springer-Verlag Berlin Heidelberg 2017

Abstract The influence of gas high-temperature hot corrosion (HTHC) pre-exposure on low-cycle fatigue (LCF) behavior was characterized for the directionally solidified (DS) Ni-based superalloy DZ125. Fatigue tests were carried out at 850 °C in the pre-exposed and unexposed specimens for 2, 15 and 25 h. Experimental results show that the porous corrosion scale and γ' -depleted layer formed in gas hot corrosion condition alter the crack initiation mechanisms of the superalloy. Fatigue cracks of the pre-exposed specimens originate from multiple surface locations where spalling of the corrosion products occur, while nucleation of unexposed specimen begins in the defects close to the surface. There is a significant reduction in LCF behavior for pre-exposed specimens in comparison with unexposed specimens.

Keywords Low-cycle fatigue; Hot corrosion; Pre-exposure; Burner rig; Ni-based superalloy

1 Introduction

Directionally solidified (DS) nickel-based superalloy, which has superior fatigue and creep properties in a large temperature range compared with the conventional polycrystalline Ni-based superalloy, is used for modern aero-engine turbine hot section components, such as turbine blades.

During the aero-engine service in a marine environment, the turbine blades are subject to high-temperature environmental attack due to the ingested salt from sea water and saline atmosphere in combination with sulfur, vanadium and other alkali metals in aviation fuel [1, 2]. The molten salts in the prevailing temperature generally induce two types of hot corrosion: Type I (high-temperature hot corrosion, HTHC) and Type II (low-temperature hot corrosion, LTHC) [1, 3]. Meanwhile, the blades also experience significant temperature and stress fluctuation that lead to localized and small plastic strains. Hence, the components are designed against low-cycle and low-frequency fatigue [4]. The interaction of hot corrosion and low-cycle fatigue (LCF) often determines the ultimate failure of turbine blades. Therefore, the investigations on hot corrosion and LCF interaction have been reported [5–10]. However, these previous studies were generally carried out under the air hot corrosive condition. Few scholars have focused on the LCF behavior of DS superalloy pre-exposed in gas HTHC environment that simulated the actual service condition of the DS turbine blades. This mainly owes to the experimental difficulties and high costs associated with conducting the experimentations.

The objective of this study is to provide a better understanding about how gas hot corrosion prior exposure influences LCF behavior of DS nickel-based superalloy typically used for aero-engine turbine blades material. Fatigue tests were carried out in the pre-exposed and unexposed specimens for different time.

2 Experimental

2.1 Materials and specimen preparation

The DS nickel-based superalloy DZ125 was investigated after the following heat treatment: 1180 °C/2 h + 1230 °C/

H.-Y. Qi, J.-S. Yang, X.-G. Yang*, S.-L. Li
School of Energy and Power Engineering, Beihang University,
Beijing 100191, China
e-mail: yxg@buaa.edu.cn

H.-Y. Qi, X.-G. Yang
Collaborative Innovation Center of Advanced Aero-Engine,
Beijing 100191, China

3 h/AC + 1100 °C/4 h/AC + 870 °C/20 h/AC (AC: air cooling). The nominal chemical composition of DZ125 alloy (in wt%) is: balance Ni, 0.100 C, 8.900 Cr, 10.000 Co, 7.000 W, 2.000 Mo, 5.200 Al, 0.900 Ti, 3.800 Ta, 1.500 Hf and 0.015 B.

Figure 1 shows the geometry of L-oriented specimen for LCF tests. The [001] orientation of DS grains is parallel to the axis of specimen, i.e., the loading direction corresponds approximately to the principal orientation. To exclude surface machining defects, the gauge sections of all solid specimens were fine-ground with 400, 800 and 1200 grit SiC sand paper successively before testing [11].

2.2 Pre-exposure LCF testing

The effects of prior high-temperature-fuel-gas hot corrosive exposure on LCF behavior were investigated using pre-exposure time (t_{pre}) of 2, 15, 25 h and pre-temperature (T_{pre}) of 850 °C. In all cases of hot corrosion prior exposure, a dried mixture salt coating of about $5 \text{ mg}\cdot\text{cm}^{-2}$ (75 wt% Na_2SO_4 + 25 wt% NaCl) on the surface of each tested specimen was achieved via several sprays, and a fine salt distribution on the specimen surface was observed, as exhibited in Fig. 2a. Prior exposure tests were carried out using a self-designed burner rig operating at atmospheric pressure. This burner rig was fired using an aviation fuel (RP-3). After prior exposure treating, all specimens were cooled to room temperature and prepared for LCF tests. Moreover, the LCF behavior of some bare specimens unexposed was used to compare with that of the pre-exposed specimens.

The high-temperature LCF experiments on pre-exposed and unexposed specimens were conducted at 850 °C on servo-hydraulic material fatigue testing system (Shimadzu-EHF-EM100) with 100 kN under total load-control mode, while mechanical stress cycle had a triangular shape with a stress ratio R of 0, a constant stress rate of $400 \text{ MPa}\cdot\text{s}^{-1}$ and the maximum stress (σ_{max}) of 680 MPa. During the tests, the continuous temperature was measured with external thermocouples attached to the specimen to keep the temperature variation of 2 °C within a gauge section.

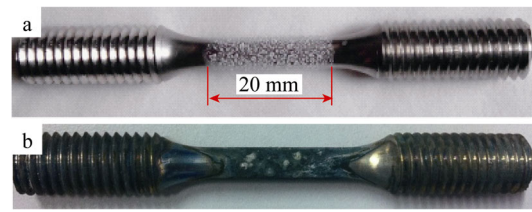


Fig. 2 Macrophotographs showing specimen prior to fatigue testing: **a** salt-coated and **b** after exposed to hot corrosion environment at 850 °C for 15 h

2.3 Microstructural examinations

The cross-sectional morphologies and fracture surfaces of all tested specimens were examined under scanning electron microscopy (SEM, JEOL JSM-6010) to study the effects of HTHC pre-exposure on LCF behavior of superalloy DZ125. The composition of corrosion products was analyzed using energy-dispersive spectrometer (EDS) equipped to SEM.

3 Results and discussion

3.1 Surface layer characterization

High-temperature hot corrosion generally consists of two stages: the incubation period and accelerated corrosion attack period [12]. Meanwhile, the corrosion process contains oxidation reaction. Strictly speaking, high-temperature oxidation is only one type of high-temperature corrosion. Therefore, a protective $\text{Cr}_2\text{O}_3/\text{Al}_2\text{O}_3$ scale is usually formed in the initial stage of hot corrosion, but is subsequently broken due to the attack of molten salt on the surface of specimen. And then, a porous corrosion layer is generated on the external surface of specimen, which cannot provide an effective protect to suppress corrosive elements penetration inward [13, 14]. Further, as the result of Al and Ti being stripped from γ' particles, the γ' -depleted zone, which can be also named as the sulfidation layer due to the

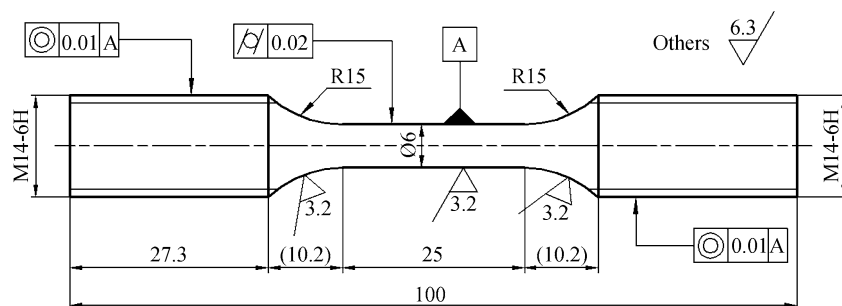


Fig. 1 Shape and dimensions of L-oriented specimen for LCF tests (all dimensions in mm)

existence of chromium sulfides, is generally found beneath the corrosion scale.

Figure 2b shows that the prior HTHC exposure alters the sample surface which is very rough and has a greenish appearance. The greenish color may be a macroscopic feature of HTHC products [3, 15]. The high magnification view of the surface condition of pre-exposed and unexposed fatigue specimens scanned by SEM is shown in Fig. 3. The prior gas hot corrosion exposure influences the microstructure of specimen surface; however, the pre-exposed specimen surface is rough, while the unexposed is smooth. Two different regions on the surface of pre-exposed specimen are marked as Regions B and C. The compositions of the major corrosion products are listed in Table 1. Owing to just slight spallation on Region C, the surface produces mainly consist of Al_2O_3 and NiO. Region B is mostly composed of a porous and loose Co and Ni oxides. It indicates that the specimen surface may occur local corrosion damage after prior gas hot corrosion exposure, which may be attributed to the nonuniform salt coating surface under fuel gas flow.

Cr and Al contents in the exposed Region B, as shown in Table 1, are less than those in the initial state. Once the sample is subjected to subsequent fatigue loading, corrosion product spallation may locally occur, as shown in Fig. 3. The corrosion scale prior to fatigue cycling alters

Table 1 Elemental content of DZ125 alloy in Regions A, B, and C of Fig. 3

Elements	Region A		Region B		Region C	
	w/wt%	x/at%	w/wt%	x/at%	w/wt%	x/at%
O	21.45	46.74	21.73	49.09	21.77	45.82
Al	11.03	14.25	3.12	4.18	15.27	19.05
Ti	0.81	0.59	0.81	0.61	1.48	1.04
Cr	10.41	6.98	5.11	3.55	7.02	4.55
Co	9.09	5.38	22.11	13.56	7.98	4.56
Ni	41.61	24.71	47.11	29.00	41.36	23.72

the diffusion and damage processes locally at the surface and influences the fatigue life and fracture behavior of superalloy.

3.2 Specimen sections and fractograph

The most conspicuous effects of exposing superalloy DZ125 under gas HTHC condition can be categorized as those affecting either the surface or the subsurface of the microstructure. The crack initiation behavior of DZ125 alloy is influenced not only by the corrosion scale, but also the γ' -depleted layer. After LCF tests, the thicknesses of the corrosion scale and the γ' -depleted layer of the pre-

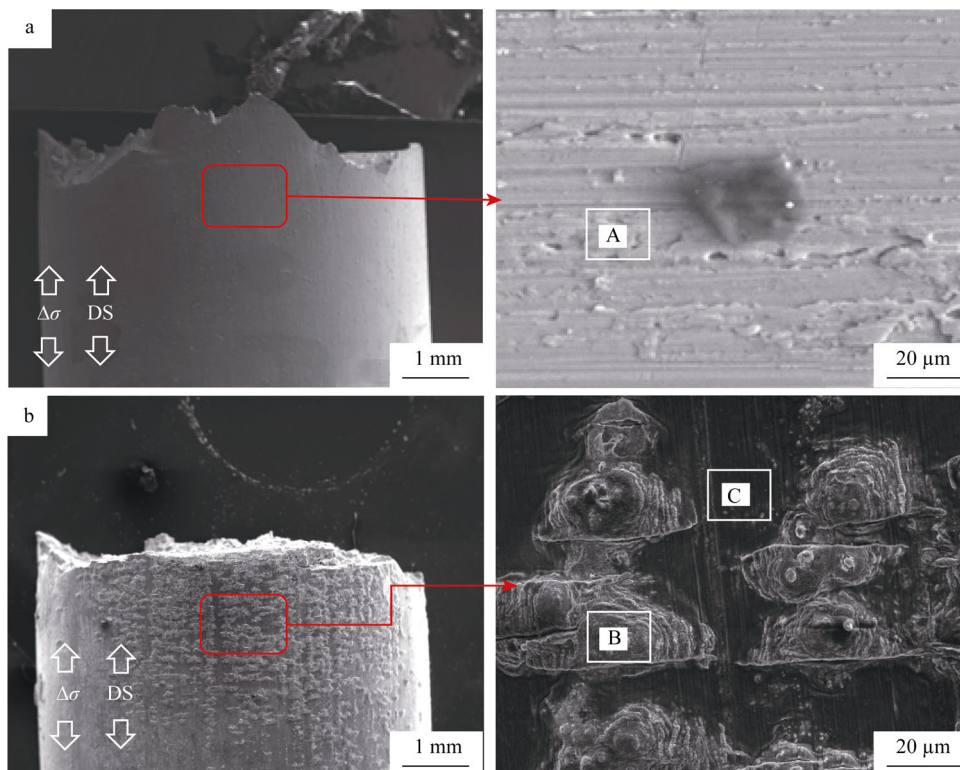


Fig. 3 SEM images of **a** surface of unexposed specimens (850 °C; $R = 0$; $\sigma_{max} = 680$ MPa) and **b** specimens of a prior hot corrosion exposure (850 °C; $R = 0$; $\sigma_{max} = 680$ MPa; $t_{pre} = 25$ h; $\Delta\sigma$: applied load)

exposed specimens are approximately 100 and 13 μm , respectively, as shown in Fig. 4. However, the fatigue crack of superalloy is generally prone to initiating at the material surface or inner defect of material [16]. Since surface degradation is more aggressive in prior hot corrosion condition, cracks are easier to generate on the specimen surface and subsequently passed through the γ' -depleted layer into the substrate. The presence of the corrosion scale and γ' -depleted layer influences the crack initiation mechanisms.

The SEM images of the fatigue fracture surface features of pre-exposed and unexposed specimens are shown in Fig. 5. The fracture surface of unexposed specimens (bare DZ125 alloy) is flat (Fig. 5a), while that of pre-exposed samples is relatively uneven (Fig. 5b). Spallation is obviously observed on the outer surface of the specimens subjected to pre-exposure and low-cycle loading at elevated temperatures, but is not obvious on the surface of unexposed specimen. The features of Region A marked in Fig. 5a, b may be produced in the crack initiation and early propagation stages. The period has a fairly slow crack propagation velocity, leading to generate a relatively smooth fracture surface and fatigue striations, and takes a large portion of the total fatigue life.

For the unexposed specimen, the fatigue cracks are subsurface-initiated, and one noticeable fatigue source could be found on the fracture surface. The main crack sources are situated in the margin of fracture surface where casting defects exist. Stress concentration caused by defects at elevated temperature leads to subsurface crack initiation and accelerates the crack growth. It is demonstrated that subsurface-initiated cracking is the dominant damage mechanism despite the cracks occurred on the specimen surface.

Conversely, based on the fracture surfaces of pre-exposed specimens, nucleation of specimen cracks generally begins in multiple surface locations where spalling of the

corrosion products has occurred because of prior exposure. In a previous pre-exposure study using DS GTD-111 [17], the fatigue cracks are nucleated by coalescence of micro-cracks that form during the pre-exposure period, which may be the dominant mechanism facilitating damage under prior exposure condition. Therefore, this finding also verifies that prior gas exposure alters the crack initiation mechanism locally.

3.3 Fatigue life

Figure 6 compares the pre-exposed and unexposed effects on the fatigue life of superalloy DZ125. It indicates that the specimens pre-exposed in a gas hot corrosion condition have lower fatigue life than that of unexposed samples. Pre-exposing the alloy in burner rig has detrimental effect on life. Increasing the pre-exposure time has the effect of increasing the corrosion penetration, which further decreases fatigue life. Table 2 exhibits that the lives of pre-exposed specimens for 2, 15 and 25 h drop approximately by 41%, 62% and 83%, respectively, compared with that of unexposed specimen, showing that the trend of fatigue life is virtually a straight line down.

In the previous studies involving prior exposure, pre-exposure results in the reduction of alloy fatigue lives [17–19]. However, the life reduction is normally a direct consequence of the degraded microstructure and alloy mechanical properties. Antolovich et al [18] imply that the γ' -depleted zone developed via prior exposure had detrimental effects on the subsequent fatigue life of alloy. At elevated temperature, the Vickers hardness of γ' -depleted layer is less than that of the matrix material [20]. It suggests that the mechanical degradation may be occurred in the layer [18]. Therefore, pre-exposing the sample in gas HTHC environment leads to deeper ingress of the corrosion layer and the γ' -depleted layer compared with the unexposed condition, eventually leading to the reduction of

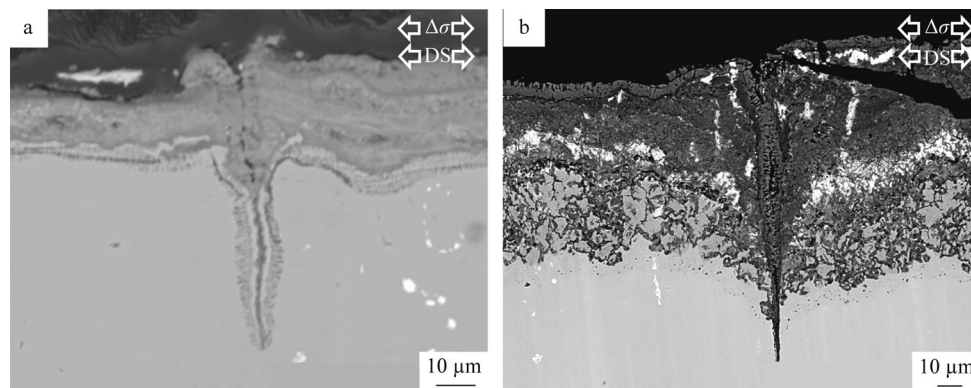


Fig. 4 Backscattered electron (BSE) images of longitudinal sections of LCF specimens under different conditions: **a** unexposed specimens and **b** pre-exposed 15 h in hot corrosion environment

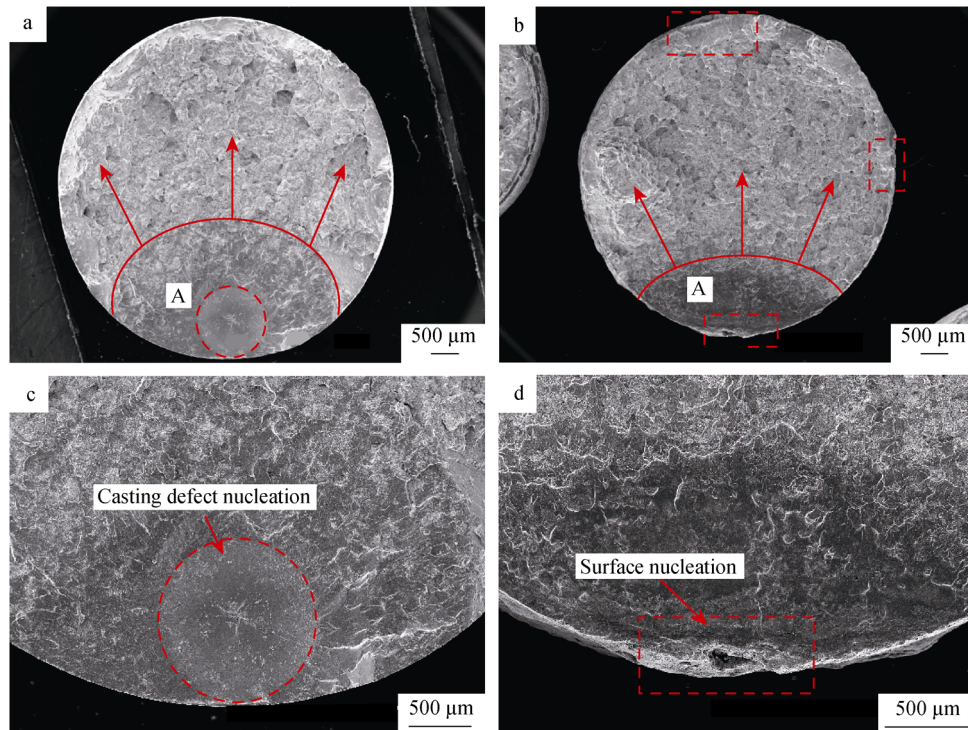


Fig. 5 SEM images of fatigue fracture surface features: **a, c** unexposed specimens, showing single crack origin and crack nucleated at internal defect; **b, d** pre-exposed specimens, 15 h, showing multiple crack origins and crack nucleated at surface (850 °C; $R = 0$; $\sigma_{max} = 680$ MPa)

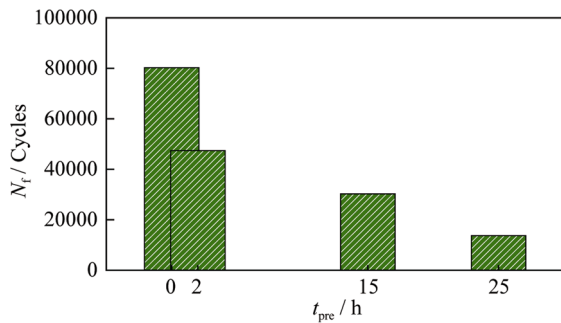


Fig. 6 Histogram of fatigue life for pre-exposed and unexposed specimens with different prior exposure time subjected to maximum stress of 680 MPa at 850 °C

Table 2 Reduction rate (RR) and LCF fatigue life (N_f) of pre-exposed and unexposed DZ125 samples

Status	Time/h	$N_f/cycles$	RR/%
Unexposure	–	80,270	–
Pre-exposure	2	47,365	40.99
	15	30,261	62.30
	25	13,729	82.89

the net bear section. In addition, as discussed in Sect. 3.2, the porous corrosion layer is prone to cracking. Thus, the LCF life severely decreases for pre-exposed specimen.

4 Conclusion

The porous corrosion scale and γ' -depleted layer of the specimen pre-exposed in gas HTHC condition are mechanically degraded layers for the materials, which alter the diffusion and damage processes locally at the surface and have a detrimental influences on the fatigue life and fracture behavior of superalloy.

Prior exposure influences the crack initiation mechanisms. Fatigue cracks of the unexposed specimens originate from the defects close to the surface and propagate inward, and subsurface-initiated cracking is the dominant damage mechanism, whereas nucleation of pre-exposed specimen cracks begins in multiple surface locations where spalling of the corrosion products occurs. These cracks were nucleated by coalescence of microcracks that had formed during the pre-exposure period.

From the LCF tests conducted at 850 °C, it is established that there is a significant reduction in LCF behavior for pre-exposed specimens in comparison with bare specimens. The life of pre-exposed specimens for 2, 15, and 25 h drops approximately by 41%, 62% and 83%, respectively, compared with the unexposed specimen life. The trend of fatigue life is virtually a straight line down with the pre-exposure time. The life reduction is normally a direct consequence of the degraded microstructure and alloy mechanical properties.

Acknowledgements This study was financially supported by the National Natural Science Foundation of China (No. 51571010) and the National Basic Research Program of China (No. 2015CB057400).

References

- [1] Pollock TM, Tin S. Nickel-based superalloys for advanced turbine engines: chemistry, microstructure and properties. *J Propul Power*. 2006;22(2):361.
- [2] Sahm PR, Speidel MO, Woodford DA. High-temperature materials in gas turbines. *J Eng Mater Technol*. 1975;1:94.
- [3] Eliaz N, Shemesh G, Latanision RM. Hot corrosion in gas turbine components. *Eng Fail Anal*. 2002;9(1):31.
- [4] Rapp RA. Hot corrosion of materials. *Pure Appl Chem*. 1990;62(1):113.
- [5] Carter TJ. Common failures in gas turbine blades. *Eng Fail Anal*. 2005;12(2):237.
- [6] Guo J, Ranucci D, Picco E. Low cycle fatigue behaviour of cast nickel-base superalloy IN738LC in air and in hot corrosive environments. *Mater Sci Eng*. 1983;58(1):127.
- [7] Sahu JK, Gupta RK, Swaminathan J, Pauloseb N, Mannanb SL. Influence of hot corrosion on low cycle fatigue behavior of nickel base superalloy SU 263. *Int J Fatigue*. 2013;51(2):68.
- [8] Mahobia GS, Sudhakar RG, Antony A, Chattopadhyay K, NC, Santhi Srinivas NC, Singh Vakil. Effect of salt coatings on low cycle fatigue behavior of nickel-base superalloy GTM-SU-718. *Proc Eng*. 2013;55:830.
- [9] Mahobia GS, Paulose N, Mannan SL, Sudhakara RG, Chattopadhyaya K, Santhi Srinivasa NC, Singha Vakil. Effect of hot corrosion on low cycle fatigue behavior of superalloy IN718. *Int J Fatigue*. 2014;59(2):272.
- [10] Guo J, Ranucci D, Picco E, Strocchi PM. Effect of environment on the low cycle fatigue behaviour of cast nickel-base superalloy IN738LC. *Int J Fatigue*. 1984;6(2):95.
- [11] Saunders S, Nicholls J. Hot salt corrosion test procedures and coating evaluation. *Thin Solid Films*. 1984;119(3):247.
- [12] Ma J, Jiang SM, Gong J, Chao S. Behaviour and mechanisms of alkali-sulphate-induced hot corrosion on composite coatings at 900 °C. *Corros Sci*. 2012;58:251.
- [13] Qiao Y, Guo X, Li X. Hot corrosion behavior of silicide coating on an Nb–Ti–Si based ultrahigh temperature alloy. *Corros Sci*. 2014;91:75.
- [14] Zheng L, Zhang MC, Dong JX. Hot corrosion behavior of powder metallurgy Rene95 nickel-based superalloy in molten NaCl–Na₂SO₄ salts. *Mater Des*. 2011;32(4):1981.
- [15] Kosieniak E, Biesiada K, Kaczorowski J, Innocenti M. Corrosion failures in gas turbine hot components. *J Fail Anal Prev*. 2012;12(3):330.
- [16] Yang XG, Dong CL, Shi DQ, Zhang L. Experimental investigation on both low cycle fatigue and fracture behavior of DZ125 base metal and the brazed joint at elevated temperature. *Mater Sci Eng A*. 2011;528(22):7005.
- [17] Gordon AP, Neu RW, Well DL. Effect of pre-exposure on crack initiation life of a directionally solidified Ni-base superalloy. *Int J Fatigue*. 2009;31(2):393.
- [18] Antolovich SD, Domas P, Strudel JL. Low cycle fatigue of René 80 as affected by prior exposure. *Metall Trans A*. 1979;10(12):1859.
- [19] Nazmy M, Denk J, Baumann R, Künzler A. Environmental effects on tensile and low cycle fatigue behavior of single crystal nickel base superalloys. *Scripta Mater*. 2003;48(5):519.
- [20] Barbosa C, Nascimento JL, Caminha IMV, Abud IC. Microstructural aspects of the failure analysis of nickel base superalloys components. *Eng Fail Anal*. 2005;12(3):348.